ECCOMAS Thematic Conference on Multibody Dynamics
July 24 - 28, 2023, Lisbon, Portugal

The geometrically exact beam model with a normalized quaternion discretization

Paul Wasmer[1], **Peter Betsch**[1]

[1] Institute of Mechanics
Karlsruhe Institute of Technology
Otto-Amman-Platz 9, 76131 Karlsruhe, Germany
paul.wasmer@kit.edu / peter.betsch@kit.edu

ABSTRACT

The most significant beam model for large deformations is the geometrically exact beam, whose configuration manifold is a complex mathematical structure represented by $\mathbb{R} \times SO(3)$. To solve the partial differential equation that describes the beam's behavior, the Finite Element Method (FEM) is typically employed. However, discretizing $SO(3)$ using finite elements requires an alternative approach due to its matrix group structure, which cannot be directly discretized with the classical additive finite element approach. Unit quaternions offer an interesting parametrization of $SO(3)$ and are therefore utilized. Although unit quaternions have a complex mathematical structure, their unit length can be maintained using a normalization technique while applying an additive discretization technique. We incorporate this innovative approach with the Isogeometric Analysis, which is known to offer advantages over classical FEM with Lagrangian elements, particularly for dynamic problems.

Keywords: geometrically exact beam, Simo-Reissner beam, quaternion, geodesic finite element,isogeometric analysis.

1 Introduction

Beam models play an important role in the efficient simulation of slender structures in many different fields of engineering. The most important beam model for large displacements is the so-called geometrically exact beam also often referred to as Simo-Reissner beam [1, 2].
The configuration manifold of the beam model is given by $\mathbb{R}^3 \times SO(3)$ as it describes the position of the centerline as well as the orientation of the beam's cross-section. The partial differential equation describing the behavior of the beam is usually solved with the help of the Finite Element Method (FEM). So it becomes necessary to discretize the special orthogonal group $SO(3)$ in a finite element sense.
A finite element discretization of the special orthogonal group is rather difficult as $SO(3)$ is not an abelian, additive group but a matrix group under multiplication [3]. To obtain an optimal convergence behavior, when discretizing non-linear manifolds such as the $SO(3)$ with finite elements the geometric structure of the manifold, must be conserved [4, 5]. To circumvent this problem Simo [2] proposed a discretization on the level of incremental rotations, again a linear space as it coincides with the tangent space $TM_{SO(3)}$ of $SO(3)$. However, it was shown by Crisfield and Jelenić [6] that this leads to a path-dependence behavior.
Another approach was proposed in [7, 8] where the so-called directors, a moving frame, are discretized. The directors are discretized additively, so in a classical finite element sense, without additional effort. Hereby it becomes necessary to introduce constraints to ensure the mutual orthogonality as well as normality of the directors, which leads to a rather stiff behavior and is, thus, prune to locking. Furthermore, it leads to a large increase in the unknowns of the problem. As shown in [9, 10] an additional projection using the polar decomposition is necessary to conserve the underlying structure of the directors, which is $SO(3)$. Otherwise, the convergence behavior of higher order discretization cannot be expected to be optimal. In the polar decomposition, an

eigenvalue problem has to be solved, which is very costly in terms of computational effort.
The use of unit quaternions for the parametrization of $SO(3)$ presents an interesting alternative [11]. They represent an extension to the complex numbers and like them, they can be used to parametrize rotations. But instead of two-dimensional rotations, quaternions of unit length are used to display rotation in the three-dimensional space. They are often employed in computer graphics as even though they do not represent the minimal set of coordinates can be used very efficiently to compute tensors from $SO(3)$ as there is no need to evaluate trigonometric functions while doing so. To obtain an optimal convergence behavior, when discretizing unit quaternion with finite elements the geometric structure S^3, which is parametrized by them, should be conserved [4, 5]. This results in the need to conserve the length of the unit quaternions at every point of the discretized domain.
A possibility to conserve complex structures of arbitrary Riemann manifolds are the so-called geodesic finite elements (GFE) [4, 12], for which optimal convergence behavior is not just shown numerically but is proven analytically [5]. They cover all kinds of rotational parametrizations due to their general formulation. The approach published by Crisfield [6] falls into this category as well as the spherical linear interpolation (SLERP) algorithm [11], the standard approach in computer graphics. In [4] this element formulation is applied to the geometrically exact beam formulation in a quaternion formulation. GFEs have, however, not the structure of a classical finite element discretization, which makes the implementation more difficult. Further, it leads to the need to evaluate trigonometric functions multiple times in each step of the Netwon iteration making them computationally costly.
Another possibility was proposed by in [8] and in a more general approach in [9, 10]. Here, the unit length of quaternions can be assured using a projection, while still applying an additive discretization technique. In [10] the convergence behavior of these so-called projection-based elements is investigated analytically and numerically. It is found to be optimal. Furthermore, it is shown that the projection-based approach for S^3 conserves the objectivity of the discretized equations. In [13] this approach is applied to a slightly different problem of the geometrically exact shell formulation, where it is used to discretize the unit sphere S^2. We apply this approach again to the geometrically exact beam formulation because even though it was applied in [8] to the geometrically exact beam formulation it is not covered in great detail.
Regardless of various publications [14, 15] which deal with quaternions in the geometrically exact beam formulations it is usually not reformulated in terms of linear algebra. However, for an efficient numerical implementation of the model, this is crucial. So we present the beam formulation in terms of linear algebra and apply the projection-based discretization method to it.
In the literature, it is often shown that the Isogeometric Analysis (IGA) is advantageous over the classical FEM with Lagrangian elements, especially for dynamic problems [16]. We thus apply the IGA to the quaternion formulation of the geometrically exact beam. However, the proposed model can be applied to Lagrangian shape functions in the same manner.
An outline of the rest of the paper is as follows. In Sec.2 we introduce the basic of quaternions as well as unit quaternions and how they can be used to display rotations. Further, we discuss the problem of the discretization of the manifold given by the unit quaternions. In Sec. 3 we give a very short introduction to the geometrically exact beam formulation and apply the results obtained above to the formulation. Numerical examples showing promising results follow in Sec. 4. At the end, we give a short conclusion in Sec. 5.

2 Quaternions

The space of quaternions $\mathbb{H}$ can be seen as an extension of the space imaginary numbers $\mathbb{C}$. Like the imaginary numbers a quaternion $\mathbb{q} \in \mathbb{H}$ consist of a scalar real part $q_0 \in \mathbb{R}$ and an imaginary part also called vector part. A quaternion is constructed with the help of the imaginary basis $(\mathrm{i},\mathrm{j},\mathrm{k})$ as

$$\mathbb{q} = q_0 + q_1\mathrm{i} + q_2\mathrm{j} + q_3\mathrm{k} = (q_0, \mathrm{q}) \, , \qquad (1)$$

where $q_1, q_2, q_3 \in \mathbb{R}$. From here on, we apply the notation with the brackets. Standard operations like the addition, the scalar product, or the multiplication with a scalar can be applied to quaternions as with vectors in $\mathbb{R}^4$. However, a new algebra is introduced for the multiplication of two quaternions. It can be written as

$$\mathbb{q} \circ \mathbb{p} = (q_0 p_0 - \mathrm{q} \cdot \mathrm{p}, q_0 \mathrm{p} + p_0 \mathrm{q} + \mathrm{q} \times \mathrm{p}) = \mathbb{v} \in \mathbb{H}, \tag{2}$$

where $\mathrm{q} \cdot \mathrm{p} = q_i p_i$ is the standard scalar product between two vectors. We apply the Einstein notation for double indices in this work, where lower roman indices i, j, k run from 1 to 3, upper roman indices I, J, K from 1 to 4 and Greek letter indices α, β as used in Sec. 3 take values 1 and 2. In contrast to the vectors from the $\mathbb{R}^n$ quaternions $\mathbb{q}, \mathbb{p} \in \mathbb{H}$ are closed under the product $\mathbb{q} \circ \mathbb{p} = \mathbb{v} \in \mathbb{H}$. Due to the last term involving the cross product the quaternion product is not commutative.
Similar to imaginary numbers the conjugate of a quaternion is defined by

$$\bar{\mathbb{q}} = (q_0, -\mathrm{q}) \,. \tag{3}$$

The norm of a quaternion is defined as for a vector of $\mathbb{R}^4$

$$\|\mathbb{q}\| = \sqrt{\mathbb{q} \cdot \mathbb{q}} = \sqrt{q_0^2 + q_1^2 + q_2^2 + q_3^2}\,, \tag{4}$$

and for each quaternion, an inverse can be constructed in the following way

$$\mathbb{q}^{-1} = \frac{1}{\|\mathbb{q}\|} \bar{\mathbb{q}} \,. \tag{5}$$

2.1 Unit quaternions

Quaternions of unit length are of special interest as they can be used to display rotation very efficiently. The space of unit quaternions is called $\mathbb{H}_1$

$$\mathbb{H}_1 = \{\mathbb{q} \in \mathbb{H} \,|\, \|\mathbb{q}\| = 1\} \,. \tag{6}$$

They form a parametrization of the unit sphere S^3 in $\mathbb{R}^4$, which is defined by

$$S^3 = \{\mathbb{q} \in \mathbb{H}_1\} \,. \tag{7}$$

Unit quaternions have a Lie group structure, with the quaternion multiplication $\circ$ as defined in Eq. (2) as the group action. Taking the time derivative of the unit constraints

$$\dot{\mathbb{q}} \cdot \mathbb{q} + \mathbb{q} \cdot \dot{\mathbb{q}} = 0 \,. \tag{8}$$

and evaluating the equation at the groups' identity $\varepsilon = (1, 0)$ reveals that admissible velocities that lie in the tangent space are pure quaternions with a real part equal to zero

$$T_\varepsilon S^3 = s^3 = \{\mathbb{v} \in \mathbb{H}_0 \,|\,, \mathbb{v} = (0, \mathrm{v})\} \,. \tag{9}$$

This is also called the Lie algebra denoted by s^3. It is isomorph to $\mathbb{R}^3$. The Lie algebra can be mapped to the unit sphere S^3 with the exponential map

$$\exp((0, \frac{1}{2}\mathrm{v})) = \cos(\frac{1}{2}\|\mathrm{v}\|)(1, 0) + \frac{\sin(\frac{1}{2}\|\mathrm{v}\|)}{\|\mathrm{v}\|}(0, \mathrm{v}) \,, \tag{10}$$

which is very similar to the Euler formula for complex numbers ($\exp(i\phi) = \cos(\phi) + i\sin(\phi)$). Every rotation in 3D can be defined by a rotation angle $\phi = \|\mathrm{v}\|$ and an axis of rotation given by a unit vector $\mathrm{v}/\|\mathrm{v}\|$ as stated by Euler's theorem. A rotation of a vector $\mathrm{v} \in \mathbb{R}^3$ with the help of the quaternion algebra can be written as

$$(0,\mathrm{v}') = \mathbb{q} \circ (0,\mathrm{v}) \circ \bar{\mathbb{q}}\,, \tag{11}$$

where v' is then the resulting rotated vector. The division by the factor 2 in Eq. (10) accounts for the effect of the two quaternions in Eq. (11). Even though the rotation of an element v of $\mathbb{R}^3$ can be written in terms of quaternion algebra. It is usually more convenient to apply the mapping from the unit sphere S^3 onto $SO(3)$ via

$$\mathrm{R}(\mathbb{q}) = (q_0^2 - \mathrm{q}\cdot\mathrm{q})\mathrm{I} + 2\mathrm{q}\otimes\mathrm{q} + 2q_0\hat{\mathrm{q}}\,, \tag{12}$$

and apply the resulting rotational tensor in a standard fashion $\mathrm{v}' = \mathrm{R}(\mathbb{q})\cdot\mathrm{v}$. Note that the same rotational tensor is given by the negative of a unit quaternion

$$\mathrm{R}(\mathbb{q}) = \mathrm{R}(-\mathbb{q})\,, \tag{13}$$

as can be seen from Eq. (12). Thus, there exists no explicit inverse mapping from $SO(3)$ to S^3 In contrast to other parametrization with rotational vectors, such as Euler angles or the Rodrigues formula, there are no trigonometric functions, which are computationally intensive when numerically evaluated, involved in Eq. (12). Thus, a parametrization of the $SO(3)$ with quaternions is very efficient. Furthermore, there exist no singularities for a quaternion representation of the $SO(3)$.

2.2 Representation of quaternions in linear algebra

For the numerical implementation, it becomes necessary to rewrite the quaternion product as defined in Eq. (2) in terms of linear algebra operations. We use the notation as introduced in [17]. For this two mappings $\mathrm{E}(\mathbb{q}),\mathrm{G}(\mathbb{q}) : \mathbb{H} \to \mathbb{R}^{3\times 4}$ are introduce

$$\mathrm{E}(\mathbb{q}) = \begin{bmatrix} -\mathrm{q} & q_0\mathrm{I}+\hat{\mathrm{q}} \end{bmatrix}\,, \qquad \mathrm{G}(\mathbb{q}) = \begin{bmatrix} -\mathrm{q} & q_0\mathrm{I}-\hat{\mathrm{q}} \end{bmatrix}\,. \tag{14}$$

We further define an operator

$$\bar{\mathrm{v}} = \begin{bmatrix} 0 & -\mathrm{v}^\top \\ \mathrm{v} & -\hat{\mathrm{v}} \end{bmatrix}\,. \tag{15}$$

mapping a vector $\mathrm{v} : \mathbb{R}^3 \to \mathbb{R}^{4\times 4}$. As before the hat denotes a skew-symmetric matrix of an axial vector $\mathrm{v} \in \mathbb{R}^3$. As shown in [17] we can then rewrite an orthogonal tensor obtained from a quaternion as

$$\mathrm{R}(\mathbb{q}) = \mathrm{E}(\mathbb{q})\mathrm{G}(\mathbb{q})^\top\,. \tag{16}$$

The time differential of Eq. (16) is thus found by applying the product rule

$$\frac{\partial \mathrm{R}(\mathbb{q})}{\partial t} = \dot{\mathrm{R}}(\mathbb{q}) = \mathrm{E}(\dot{\mathbb{q}})\mathrm{G}(\mathbb{q})^\top + \mathrm{E}(\mathbb{q})\mathrm{G}(\dot{\mathbb{q}})^\top = 2\mathrm{E}(\dot{\mathbb{q}})\mathrm{G}(\mathbb{q})^\top = 2\mathrm{E}(\mathbb{q})\mathrm{G}(\dot{\mathbb{q}})^\top\,. \tag{17}$$

where the differential after time is denoted with a dot. As we need it later to describe the beam's behavior in Sec. 3 we introduce a frame of three mutually orthogonal vectors of unit length $\mathrm{d}_i \in \mathbb{R}$

$$\mathrm{d}_i = \mathrm{R}\cdot\mathrm{e}_i\,. \tag{18}$$

We refer to the vectors d_i as directors. With the help of equation Eq. (17) when can write the directors as

$$\mathrm{d}_i = \mathrm{E}(\mathbb{q})\mathrm{G}(\mathbb{q})^\top\mathrm{e}_i = \mathrm{E}(\mathbb{q})\bar{\mathrm{e}}_i\mathbb{q}\,, \tag{19}$$

where we use the last formulation in the rest of the work. Differentiating Eq. (19) we obtain

$$\dot{\mathrm{d}}_i = \dot{\mathrm{R}}(\mathbb{q})\mathrm{e}_i = 2\mathrm{E}(\mathbb{q})\bar{\mathrm{e}}_i\dot{\mathbb{q}}\,. \tag{20}$$

2.3 Discretization of quaterions

As mentioned in Sec. 1 the discretization of a complex manifold, such as the S^3, has to be handled with great care. A standard discretization in a finite element sense with an additive structure does not preserve the manifold's structure at every point of the discretized domain. When using a discretization, which fulfills the collocation properties on the nodes such as the standard Lagrangian shape functions, it can be assured that the nodal points are on the manifold as constraints can be enforced in a strong sense. However, this does not ensure the geometric structure is conserved over the whole domain of a finite element and is not possible for an isogeometric approach of higher order, where the constraints are enforced in a weak sense. Nevertheless, for both types of shape functions the structure of the manifold is violated at integration points. Nevertheless, such an approach can be chosen, however, the convergence behavior will not be optimal [4, 12, 5]. We cannot display the $S^3 \in \mathbb{R}^4$ directly, however, a sketch illustrating a direct discretization approach is shown in Fig. 1a. The gray vectors $\mathbb{q}_1(s_1)$ and $\mathbb{q}_1(s_1)$ display the nodal values. The dotted red line indicates the discretized variable between two nodal points at s_1 and s_2 with the blue vector giving the discretized quaternion $\mathbb{q}^h$ at position s.
Another approach conserving the structure of a Riemann manifold, such as the S^3 or $SO(3)$, for a finite element discretization are the so-called GFEs as proposed by Sander [4]. Instead of choosing a classical approach, the elements are constructed using the geodesic, the shortest path, on the manifold. In [12] it is generalized to higher order discretization. This approach ensures the conservation of the geometry in every point exactly, as sketched in Fig. 1b. The optimal convergence behavior was shown analytically [5] as well as numerically [4, 12]. The approach by Crisfield [6] as well as the well-known spherical linear interpolation (SLERP) algorithm known from computer graphics [11] fall into this category. However, this approach needs to evaluate trigonometric functions at every Newton step making them costly to compute. Furthermore, it does not have an additive structure as a classical FEM approach increasing the effort for the implementation. This makes it also more devious to implement higher orders, as for the computation of higher order derivatives the product rule has to be applied multiple times. A sketch of the discretization is shown in Fig. 1b. The discretized line, indicated with the red dotted line, lies here always on the geometry of the manifold.
This is only a very short overview of discretization approaches and by no means comprehensive. However, as mentioned by Sander [4, 12] and Grohs [5, 10] the topic of finite elements conserving the structure of a manifold did so far receive not very much attention in the literature.

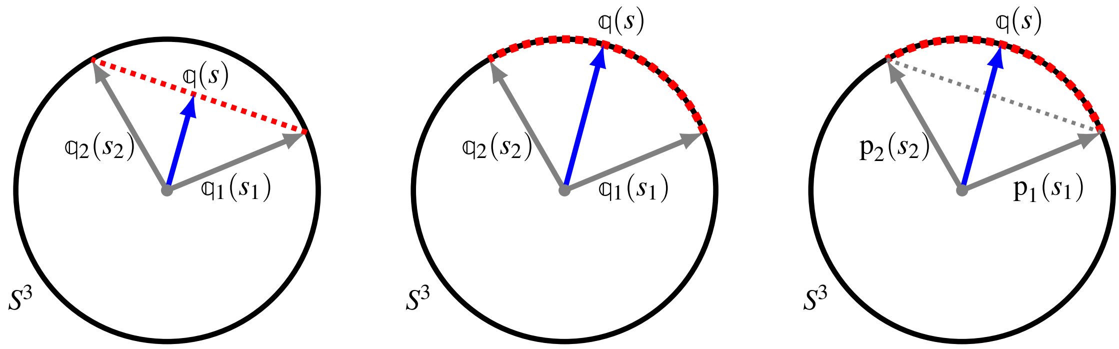

(a) Classical FEM approach (b) Geodesic finite element (c) Projection-based element

Figure 1: Sketch of different discretization approaches

2.3.1 Projection-based approach

We propose a different approach, which we think is more convenient as it resamples the classical discretization approach of finite elements. It can be applied to Lagrangian elements as well as to the isogeometric analysis. We discretize the control point (or nodal) values in a classical finite element sense

$$\mathrm{p}^h(s) = \sum_{i=1}^{n} N_{i,s}(s)\mathrm{p}_i\,, \tag{21}$$

$\mathrm{p}_i \in \mathbb{R}^4$ are control point (or nodal) values associated with the quaternions. As mentioned above this does not conserve the geometric structure of the manifold. We, therefore, project the discretized variable onto the manifold by dividing through the norm and taking the projected quantity as the physical variable. The discretized quaternion variable thus follows as

$$\mathbb{q}^h(s) = \frac{\sum_{i=1}^{n} N_i(s)\mathrm{p}_i}{\|\sum_{i=1}^{n} N_i(s)\mathrm{p}_i\|} = \mathrm{P}(\mathrm{p}^\mathrm{h}(s))\,, \tag{22}$$

where we introduced the projector $\mathrm{P}(\bullet)$. The projected quantity $\mathbb{q}^h(s)$ is the variable, which we use for the computation of the special orthogonal tensor as shown in Eq. (17). In this way, we ensure that $\mathbb{q}(s)$ is a unit quaternion at every point s and in that way always a parametrization of a tensor $\mathrm{R} \in SO(3)$. The derivative with respect to the parameter s denoted by $(\bullet)_{,s}$ follows from applying the chain rule

$$\mathbb{q}^h_{,s}(s) = \frac{\mathrm{I}_4 - \mathbb{q}^h(s) \otimes \mathbb{q}^h(s)}{\|\sum_{i=1}^{n} N_i(s)\mathrm{p}_i\|} \sum_{i=1}^{n} N_{i,s}(s)\mathrm{p}_i = \mathrm{P}'(\mathrm{p}^h(s)) \sum_{i=1}^{n} N_{i,s}(s)\mathrm{p}_i = \mathrm{P}'(\mathrm{p}^h)(s)\mathrm{p}^h_{,s}(s)\,, \tag{23}$$

where we introduced the derivative of the projector with respect to the nodal (or control point) values

$$\mathrm{P}'(\mathrm{p}^h(s)) = \nabla_{\mathrm{p}^h}\mathrm{P}(\mathrm{p}^\mathrm{h}(s)) = \frac{\mathrm{I}_4 - \mathbb{q}^h(s) \otimes \mathbb{q}^h(s)}{\|\sum_{i=1}^{n} N_i(s)\mathrm{p}_i\|}\,. \tag{24}$$

The prime $(\bullet)'$ thus denotes the derivative with respect to the discretized quantity $\mathrm{p}^h(s)$. We made use of the following connection

$$\mathbb{q}^h \otimes \mathbb{q}^h = \frac{1}{\|\sum_{i=1}^{n} N_i\mathrm{p}_i\|} \left(\sum_{i=1}^{n} N_i\mathrm{p}_i \otimes \sum_{i=1}^{n} N_i\mathrm{p}_i \right)\,. \tag{25}$$

Further, we introduce the variation of the discretized quaternion quantity

$$\delta\mathbb{q}^h(s) = \mathrm{P}'(\mathrm{p}^h(s)) \sum_{i=1}^{n} N_i(s)\delta\mathrm{p}_i = \mathrm{P}'(\mathrm{p}^h(s))\delta\mathrm{p}^h(s)\,, \tag{26}$$

where we introduced the following discretization $\sum_{i=1}^{n} N_i(s)\delta\mathrm{p}_i = \delta\mathrm{p}^h(s)$. Its derivative $\delta\mathbb{q}_{,s}$ follows from the chain rule

$$\delta\mathrm{q}^h_{,s}(s) = \Big(\mathrm{P}'(\mathrm{p}^h(s))\delta\mathrm{p}^h(s)\Big)_{,s} = \mathrm{P}''(\mathrm{p}^h(s))\mathrm{p}^h_{,s}(s)\,\delta\mathrm{p}^h(s) + \mathrm{P}'(\mathrm{p}^h(s))\,\delta\mathrm{p}^h_{,s}(s)\,, \tag{27}$$

where $\mathrm{P}''(\mathrm{p}^h)$ is the second derivative of the projector with respect to the discretized control point (or nodal) values

$$\begin{aligned} \mathrm{P}''(\mathrm{p}^h) &= \nabla_{\mathrm{p}^h}\mathrm{P}'(\mathrm{p}^h) \\ &= \frac{1}{\|\mathrm{p}^h\|^2}\Big(3\,\mathrm{q}^h \otimes \mathrm{q}^h \otimes \mathrm{q}^h - \delta_{IJ}\,\mathrm{e}_I \otimes \mathrm{e}_J \otimes \mathrm{q}^h - \delta_{IK}\,\mathrm{e}_I \otimes \mathrm{q}^h \otimes \mathrm{e}_K - \delta_{JK}\,\mathrm{q}^h \otimes \mathrm{e}_J \otimes \mathrm{e}_K\Big)\,. \end{aligned} \tag{28}$$

We here introduce a four-dimensional orthonormal bases denoted by e_I and use the dyadic product on elements with four dimensions.
The above approach was already applied by Romero [8] to the geometrically exact beam. However, as [8] is a very short contribution we feel that we can still contribute by going into greater detail.

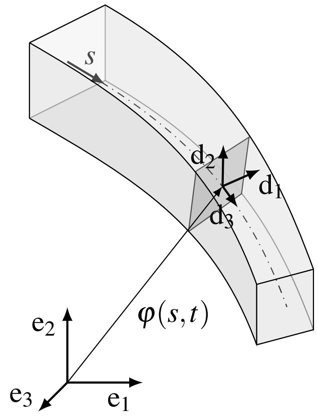

Figure 2: Sketch of the geoemtrically exact beam

3 The geometrically exact beam using quaternions

A slender structure, which is extended much longer in one dimension than in the other two, can be modeled using a beam model. The configuration of the geometrically exact beam model is described by the position of its centerline $\varphi(s,t)$ and the orientation of its cross-section plane spanned by the vectors $\mathrm{d}_\alpha(s,t)$. The coordinate $s \in [0,1]$ is the parametrization of the centerline and t is the time. Thus, every point on the beam can be described by

$$\mathrm{x}(s,t) = \varphi(s,t) + \theta(s,t) = \varphi(s,t) + \theta^\alpha \mathrm{d}_\alpha(s,t)\,, \tag{29}$$

with θ_α the convective coordinates. Note that we use the Einstein notation for double indices. Together with a third director d_3

$$\mathrm{d}_3(s,t) = \mathrm{d}_1(s,t) \times \mathrm{d}_2(s,t)\,, \tag{30}$$

the directors d_i form an orthonormal frame. The directors are of unit length and mutually orthogonal

$$\mathrm{d}_i(s,t) \cdot \mathrm{d}_j(s,t) = \delta_{ij}\,. \tag{31}$$

We thus can write the configuration $\mathbb{Q}$ of the geometrically exact beam as

$$\mathbb{Q}_{\mathrm{d}_i} = \{(\varphi, \mathrm{d}_i) : [0,L] \times [0,T] \to \mathbb{R}^3 \times \mathbb{R}^{3\times 3} \,|\, \mathrm{d}_i \cdot \mathrm{d}_j = \delta_{ij}\}\,. \tag{32}$$

However, compared with the formulation in directors the number of unknowns reduce drastically.

3.1 Kinematics of the geometrically exact beam with quaternions

Another way to express the directors is to use a special orthogonal tensor $\mathrm{R}(s,t)$ and expressed the directors as a rotation of the orthonormal basis e_i

$$\mathrm{d}_i(s,t) = \mathrm{R}(s,t) \cdot \mathrm{e}_i\,. \tag{33}$$

Here it becomes necessary to parametrize $\mathrm{R}(s,t)$ in some sense. Instead of a rotation vector, which leads to singularities, we chose a parametrization via unit quaternions. With the help of unit quaternions, we can express the beams configurations as

$$\mathbb{Q}_{\mathrm{q}} = \{(\varphi, \mathrm{q}) : [0,L] \times [0,T] \to \mathbb{R}^3 \times \mathbb{H}_1\}\,. \tag{34}$$

Eq. (29) can then be rewritten by using Eq. (19)

$$\mathrm{x}(s,t) = \varphi(s,t) + \theta^\alpha \mathrm{E}(\mathrm{q}(s,t)) \bar{\mathrm{e}}_\alpha \mathrm{q}(s,t)\,. \tag{35}$$

However, in the numerical implementation, the unit quaternions have to be represented by unit vectors $\mathrm{p} \in \mathbb{R}^4$, which leads to additional unit constraints for p. This results in the following configuration

$$\mathbb{Q}_{\mathrm{q}} = \{(\varphi, \mathrm{p}) : [0,L] \times [0,T] \to \mathbb{R}^3 \times \mathbb{R}^4 \,|\, \mathrm{p} \cdot \mathrm{p} = 1\}\,. \tag{36}$$

3.2 Strain measures with quaternions

Two strain measures define the kinematic of the beam $\Gamma = \Gamma_i \mathrm{e}_i$, accounting for shear and longitudinal strain, and $\mathrm{K} = K_i \mathrm{e}_i$ due to bending and torsion. They are well-known in the literature so we do not derive them here. However, we first show them for the director approach. With the help of the previous section, they can be rewritten in terms of quaternions

$$\Gamma_i = \mathrm{d}_i \cdot \boldsymbol{\varphi}_{,s} - \delta_{i3} = \left(\mathrm{E}(\mathbb{q})\bar{\mathrm{e}}_i\mathbb{q}\right) \cdot \boldsymbol{\varphi}_{,s} - \delta_{i3}\,, \tag{37}$$

$$\begin{aligned} K_i &= \frac{1}{2}\varepsilon_{ijk}\left(\mathrm{d}_k \cdot \mathrm{d}_{j,s} - \mathrm{d}_k \cdot \mathrm{d}_{j,s}|_{t=0}\right) \\ &= \varepsilon_{ijk}\left[\left(\mathrm{E}(\mathbb{q})\bar{\mathrm{e}}_k\mathbb{q}\right)\cdot\left(\mathrm{E}(\mathbb{q})\bar{\mathrm{e}}_j\mathbb{q}_{,s}\right) - \left(\mathrm{E}(\mathbb{q})\bar{\mathrm{e}}_k\mathbb{q}\right)\cdot\left(\mathrm{E}(\mathbb{q})\bar{\mathrm{e}}_j\mathbb{q}_{,s}\right)|_{t=0}\right]. \end{aligned} \tag{38}$$

The variation of the strain measures follows in the same fashion

$$\delta\Gamma_i = \delta\boldsymbol{\varphi}_{,s}\cdot\mathrm{d}_i + \delta\mathrm{d}_i\cdot\boldsymbol{\varphi}_{,s} = \delta\boldsymbol{\varphi}_{,s}\cdot\left(\mathrm{E}(\mathbb{q})\bar{\mathrm{e}}_i\mathbb{q}\right) + 2\left(\mathrm{E}(\mathbb{q})\bar{\mathrm{e}}_i\delta\mathbb{q}\right)\cdot\boldsymbol{\varphi}_{,s}\,, \tag{39}$$

$$\begin{aligned} \delta K_i &= \frac{1}{2}\varepsilon_{ijk}\left[\delta\mathrm{d}_k\cdot\mathrm{d}_{j,s} + \mathrm{d}_k\cdot\delta\mathrm{d}_{j,s}\right] \\ &= \varepsilon_{ijk}\left[\left(\mathrm{E}(\mathbb{q})\bar{\mathrm{e}}_k\delta\mathbb{q}\right)\left(\mathrm{E}(\mathbb{q})\bar{\mathrm{e}}_j\mathbb{q}_{,s}\right) + \left(\mathrm{E}(\mathbb{q})\bar{\mathrm{e}}_k\mathbb{q}\right)\cdot\left(\mathrm{E}(\mathbb{q}_{,s})\bar{\mathrm{e}}_j\delta\mathbb{q} + \mathrm{E}(\mathbb{q})\bar{\mathrm{e}}_j\delta\mathbb{q}_{,s}\right)\right]. \end{aligned} \tag{40}$$

3.2.1 Discretized strain measures with quaternions

Using the normalized discretization of the quaternions as introduced by Eq. (22) and Eq. (23) the strain measures are given by

$$\Gamma_i = \left(\mathrm{E}(\mathbb{q}^h)\bar{\mathrm{e}}_i\mathbb{q}^h\right)^\top \boldsymbol{\varphi}^h_{,s} - \delta_{i3}\,, \tag{41}$$

$$K_i = \varepsilon_{ijk}\left[\left(\mathrm{E}(\mathbb{q}^h)\bar{\mathrm{e}}_k\mathbb{q}^h\right)^\top\left(\mathrm{E}\left(\mathbb{q}^h\right)\bar{\mathrm{e}}_j\mathbb{q}^h_{,s}\right) - \left(\mathrm{E}(\mathbb{q}^h)\bar{\mathrm{e}}_k\mathbb{q}^h\right)^\top\left(\mathrm{E}\left(\mathbb{q}^h\right)\bar{\mathrm{e}}_j\mathbb{q}^h_{,s}\right)\Big|_{t=0}\right], \tag{42}$$

and the variation of the strain measures as

$$\delta\Gamma_i = \left(\delta\boldsymbol{\varphi}^h_{,s}\right)^\top\left(\mathrm{E}(\mathbb{q}^h)\bar{\mathrm{e}}_i\mathbb{q}^h\right) + 2\left(\delta\mathrm{p}^h\right)^\top\left(\mathrm{E}(\mathbb{q}^h)\bar{\mathrm{e}}_i\mathrm{P}'(\mathrm{p}^h)\right)^\top\boldsymbol{\varphi}^h_{,s}\,, \tag{43}$$

$$\begin{aligned} \delta K_i = &\left(\delta\mathrm{p}^h\right)^\top\varepsilon_{ijk}\Big[\left(\mathrm{E}(\mathbb{q}^h)\bar{\mathrm{e}}_k\mathrm{P}'(\mathrm{p}^h)\right)^\top\left(\mathrm{E}(\mathbb{q}^h)\bar{\mathrm{e}}_j\mathbb{q}^h_{,s}\right) \\ &+\left(\mathrm{E}(\mathbb{q}^h_{,s})\bar{\mathrm{e}}_j + \mathrm{E}(\mathbb{q}^h)\bar{\mathrm{e}}_j\mathrm{P}''(\mathrm{p}^h)\mathrm{p}^h_{,s}\right)^\top\left(\mathrm{E}(\mathbb{q}^h)\bar{\mathrm{e}}_k\mathbb{q}^h\right)\Big] \\ &+\left(\delta\mathrm{p}^h_{,s}\right)^\top\varepsilon_{ijk}\left(\mathrm{E}(\mathbb{q}^h)\bar{\mathrm{e}}_j\mathrm{P}'(\mathrm{p}^h)\right)^\top\left(\mathrm{E}(\mathbb{q}^h)\bar{\mathrm{e}}_k\mathbb{q}^h\right). \end{aligned} \tag{44}$$

Once we computed the strains and their variations, we can again write the variation of the internal strains as

$$\delta G_{\mathrm{int}} = \int_0^L \delta\Gamma\cdot\mathrm{D}_1\cdot\Gamma + \delta\mathrm{K}\cdot\mathrm{D}_2\cdot\mathrm{K}\,\mathrm{d}s\,, \tag{45}$$

with the tensors D_1 and D_2 containing the stiffness parameters computed from geometry and material properties as defined in [7].

3.3 Unit constraints

To ensure the nodal (or control point) values p_i do converge towards the unit sphere S^3 (see Sec. 3.1), we apply additional constraint

$$\Phi_{\mathrm{in}} = \mathrm{p}^h\cdot\mathrm{p}^h - 1 = 0 \tag{46}$$

In the classical FEM using Lagrange shape functions constraints are often enforced in a strong sense on the nodes. In the framework of the IGA, the constraints have to be enforced in a weak sense by integrating over the domain

$$\int_0^L \lambda^h \mathrm{G}_{\mathrm{in}} \cdot \delta \mathrm{p}^h + \delta \lambda^h \Phi_{\mathrm{in}} \,\mathrm{d}s\,, \tag{47}$$

with the constraint gradient $\mathrm{G}_{\mathrm{in}} = \nabla_p \Phi_{\mathrm{in}}$. We apply the same discretization as for the other quantities to the Lagrange multipliers.

4 Numerical validation

In this benchmark example a cantilever beam is loaded with a torque $\mathbf{M} = \begin{bmatrix} 0 & 0 & -2\pi\frac{EI}{L} \end{bmatrix} \mathbf{e}_i$ at the free end. A sketch of the problem is shown in Fig. 3a. For $M_3 = -2\pi\frac{EI}{L}$ the beam forms an exact circle. The convergence results for the displacement of the tip of the beam $\varphi(s=1)$ for different element orders are shown in Fig. 3b. The solid lines are the results of the proposed approach with the projection-based element formulation. The dashed-lines show the optimal behavior.

(a) Sketch of a cantilever beam with an end torque

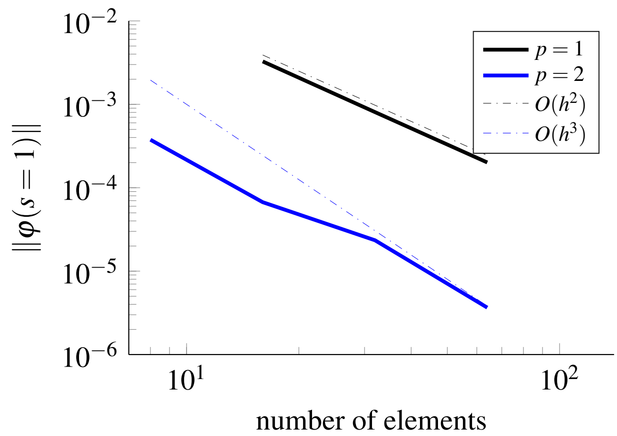

(b) Sketch of a cantilever beam with an end torque

5 Summary & Conclusion

The configuration manifold of the geometrically exact beam, given by $\mathbb{R} \times SO(3)$, has a complex structure. When solving the partial differential equations associated with the beam model with the FEM, great care has to be taken to obtain a path-independent and objective formulation. Optimal convergence behavior of the FEM solution can only be achieved if the manifolds structure is conserved. Therefore, we propose a projection-based element for a unit quaternion parametrization of $SO(3)$, which conserves the structure of the unit sphere S^3. For this purpose we introduce quaternions in a general context and show how they can parametrize a rotational tensor with linear algebra operations. We give the beams equation in terms of quaternions with this notation and we show the optimal convergence behavior for the formulation for the example of a cantilever beam roll-up.

ACKNOWLEDGMENTS

Support for P. Wasmer was provided by the Research Travel Grant of the Karlsruhe House of Young Scientists (KYHS). This support is gratefully acknowledged.

REFERENCES

[1] Reissner, E.: On one-dimensional finite-strain beam theory: The plane problem. Zeitschrift für Angew. Math. und Phys. ZAMP **23**(5) (1972) 795–804 doi:10.1007/BF01602645.

[2] Simo, J.C.: A finite strain beam formulation. The three-dimensional dynamic problem. Part I. Comput. Methods Appl. Mech. Eng **49**(1) (1985) 55–70 doi:10.1016/0045-7825(85)90050-7.

[3] Holm, D.D., Schmah, T., Stoica, C.: Geometric Mechanics and Symmetry: From Finite to Infinite Dimensions. Volume 12. Oxford University Press (2009)

[4] Sander, O.: Geodesic finite elements for cosserat rods. Int. J. Numer. Methods Eng. **82**(13) (2010) 1645–1670

[5] Grohs, P., Hardering, H., Sander, O.: Optimal a priori discretization error bounds for geodesic finite elements. Found. Comput. Math. **15**(6) (2014) 1357–1411

[6] Crisfield, M.A., Jelenic, G.: Objectivity of strain measures in the geometrically exact three-dimensional beam theory and its finite-element implementation. Proc R Soc A **455** (1999) 1125–1147

[7] Betsch, P., Steinmann, P.: Frame-indifferent beam finite elements based upon the geometrically exact beam theory. Int. J. Numer. Methods Eng. **54**(12) (2002) 1775–1788 doi:10.1002/nme.487.

[8] Romero, I.: The interpolation of rotations and its application to finite element models of geometrically exact rods. Comput. Mech. **34** (2004) 121–133

[9] Gawlik, E., Leok, M.: Embedding-based interpolation on the special orthogonal group. SIAM J. Sci. Comput. **40**(2) (2018) A721–A746

[10] Grohs, P., Hardering, H., Sander, O., Sprecher, M.: Projection-based finite elements for nonlinear function spaces. SIAM J. Numer. Anal **57**(1) (2019) 404–428

[11] Hanson, A.J.: Visualizing quaternions. Elsevier (2005)

[12] Sander, O.: Geodesic finite elements of higher order. IMA J. Numer. Anal. **36**(1) (2016) 238–266

[13] Müller, A., Bischoff, M.: A consistent finite element formulation of the geometrically nonlinear reissner-mindlin shell model. Arch. Comput. Methods Eng. **29** (2022) 3387–3434

[14] Zupan, E., Saje, M., Zupan, D.: On a virtual work consistent three-dimensional reissner–simo beam formulation using the quaternion algebra. Acta Mech. **224** (2013) 1709–1729

[15] Cottanceau, E., Thomas, O., Véron, P., Alochet, M., Deligny, R.: A finite element/quaternion/asymptotic numerical method for the 3d simulation of flexible cables. Finite Elem. Anal. Des. **139** (2018) 14–34

[16] Cottrell, J.A., Hughes, T.J.R., Bazilevs, Y.: Isogeometric Analysis - Toward Integration of CAD and FEA. John Wiley and Sons, Ltd, West Sussex (2009)

[17] Betsch, P., Siebert, R.: Rigid body dynamics in terms of quaternions: Hamiltonian formulation and conserving numerical integration. Int. J. Numer. Methods Eng. **79**(4) (2009) 444–473